NORSAR Scientific Report No. 2-2010

Semiannual Technical Summary

1 January - 30 June 2010

Frode Ringdal (ed.)

Kjeller, August 2010

6.3 A probabilistic seismic model for the European Arctic

Sponsored by the National Nuclear Security Administration

Award Nos: DE-AC52-08NA28651(NORSAR,UiO) and LL08-BAA08-38-NDD03 (LLNL)

6.3.1 Introduction

The area of interest for this study is the European Arctic, in particular the Barents Sea and surrounding regions such as the Norwegian-Greenland Sea, the Southern Eurasian Basin, Novaya Zemlya, the Kara Sea, the East European Lowlands, the Kola Peninsula and the Arctic plate boundary (Figure 6.3.1).When developing a seismic model the focus is often on finding one single best fitting model. Existing models for the region are based on approaches that try to find the model with the best fit to one or several dataset. The resulting models contain little to no information about model uncertainties. Knowledge about the robustness of features in seismic models is however beneficial for the geological interpretation of models and the reliable determination of location uncertainties for seismic events.

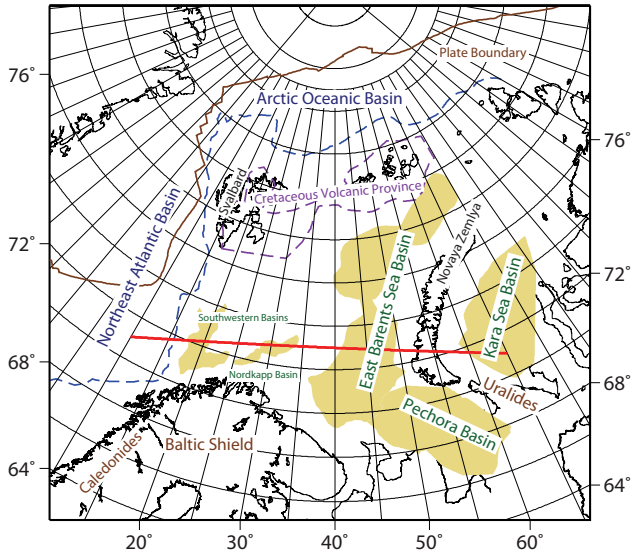

Fig. 6.3.1. Simplified tectonic map of the region after Ritzmann et al. (2007) and Bird (2003). The plate boundary is given by the brown line and continent-ocean boundary by the dashed blue line. Beige areas represent the major sedimentary basins in the Region. The cross-section along which we will examine our probabilistic model in Figure 6.3.3 is outlined in red.

Our probabilistic model differs from traditional seismic models in that it describes the posterior distribution, the ensemble of models which fit the data. The posterior distribution is proportional to the product of the prior distribution and the likelihood function. The prior distribution represents the ensemble of plausible models and the likelihood function makes models with a good fit to the data more likely than models with bad fit to the data. The data we use are thickness constraints, velocity profiles, gravity data, surface wave group velocities and body wave travel times. In this work a Markov Chain Monte Carlo (MCMC) technique is used to sample the unknown posterior distribution. This process results in 4,000 models that all fit the data.Analyzing this ensemble of models that fit the data allows to estimate a mean model and the standard deviation for the model parameters, i.e. their uncertainty. Maps of sediment thickness and thickness of the crystalline crust derived from the posterior distribution are in good agreement with knowledge of the regional tectonic setting. The predicted uncertainties, which

are equally important as the absolute values, correlate well with the variation in data coverage and data quality in the region. In addition to this a probabilistic model allows the formulation of seismic event location techniques that take into account uncertainties in the velocity model.

6.3.2 Probabilistic model

We determined an average model to compare the results of this study to other studies of the same region. The real power of a probabilistic model lies however in the fact that it describes the distribution of models that fit the data, as we will see later in the location example.

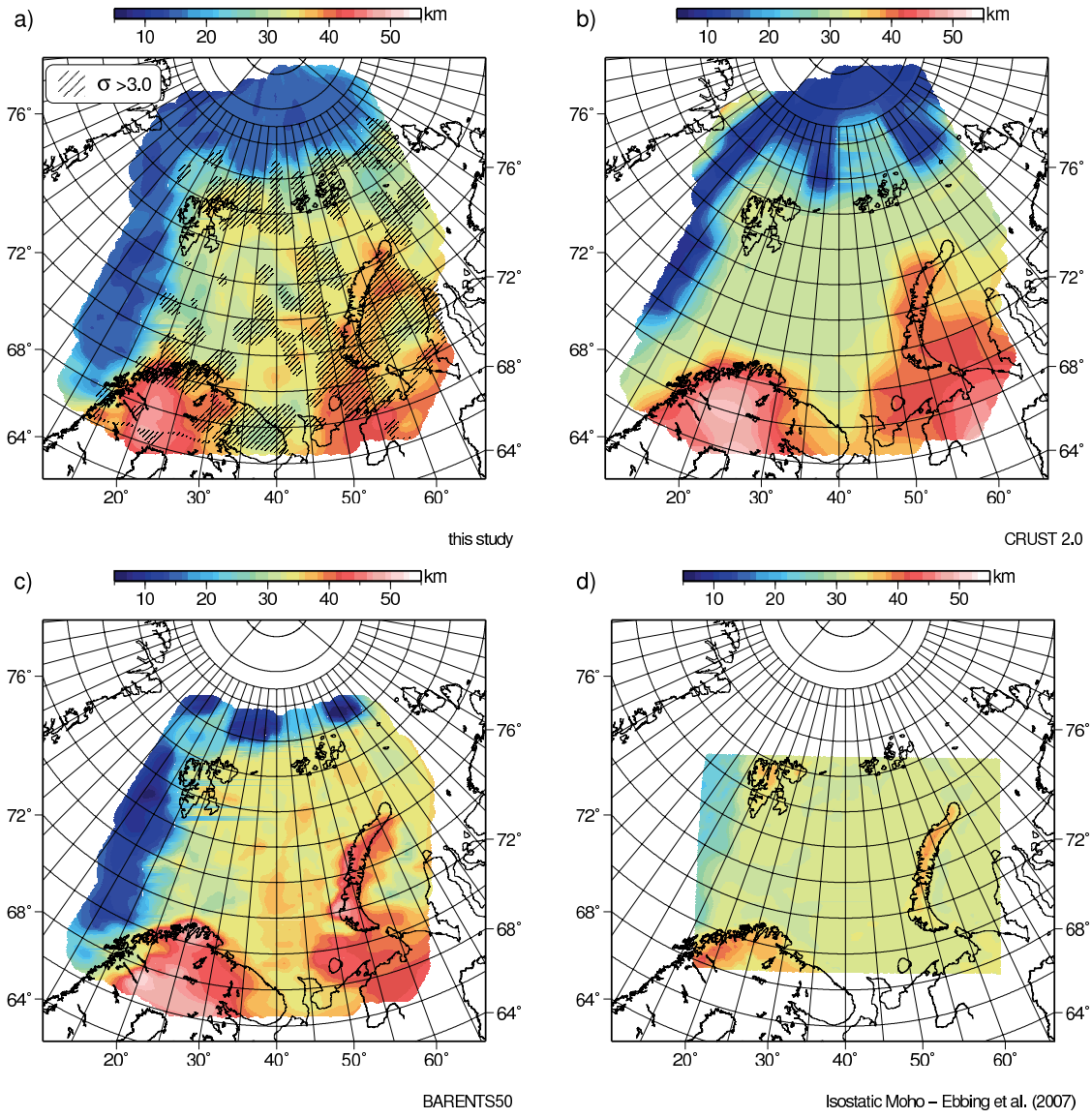

Fig. 6.3.2. Depth to Moho: a) Mean model obtained in this study, b) CRUST 2.0 after Bassin et al. (2000), c) BARENTS50 after Ritzmann et al. (2007) and d) isostatic Moho of Ebbing et al. (2007).

Figure 6.3.2 shows the depth to Moho in this study, CRUST 2.0 (Bassin et al., 2000), BARENTS50 (Ritzmann et al.,2007) and for an isostatic Moho computed by Ebbing et al. (2007). It is important to keep in mind that the different models have different spatial resolu-

tions; our model for example has a node spacing of 83 km while CRUST 2.0 uses a 2 by 2 degree grid. This makes it necessary to resample the models for this comparison. Unlike the other models our probabilistic model also provides estimates for the uncertainties, thus we can compute a standard deviation in addition to the mean of our samples of the posterior distribution. We have hatched the areas where the standard deviation on the Moho exceeds 3 km, indicating where this parameter is poorly constrained. The models are generally similar, with some notable differences. For example, most models see more complexity within the major tectonic provinces than the relative simple CRUST 2.0 model. Also, the Moho recovered by BARENTS50 appears more detailed than the Moho recovered in the present study. This comes as no surprise when one takes into account that BARENTS50 has a spatial resolution of 50 km. The models differ the most from each other around Novaya Zemlya and in the Kara Sea. Interestingly this is also where the uncertainties in the depth to Moho are generally larger than 3 km in our study. The isostatic modeling of Ebbing et al. (2007) suggests, as expected, a shallower and smoother Moho than the other, seismically-based models.

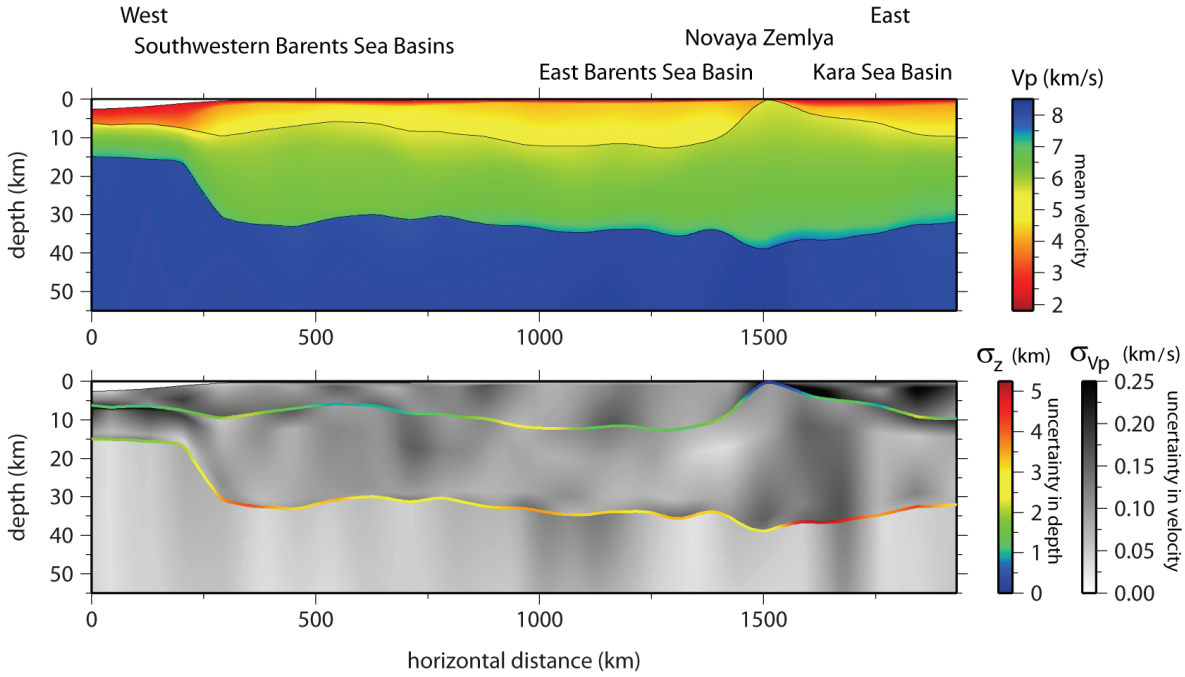

Fig. 6.3.3. West-east cross-section along the great circle path shown in Figure 6.3.1; the top panel shows Vp and the bottom panel shows the uncertainty in Vp. In the bottom panel interfaces are colored according to the uncertainty in depth.

Figure 6.3.3 shows a west to east cross-section through our probabilistic model. Unlike cross-sections further north across the western continental margin, we find a relatively rapid transition in crustal thickness and see an increase in crustal thickness associated with Novaya Zemlya. The highest uncertainty in depth to Moho lies below the Kara Sea. This is related to the weak constraints on the Moho here: gravity data and a velocity profile with a relatively high uncertainty, with no body waves sampling the Moho. We clearly recover the East Barents Sea and Kara Sea basin. The sedimentary basins in the southwestern Barents Sea, on the other hand, are only tens of kilometers wide. The node spacing of 83 km used in this study means that we cannot recover these basins. What we are able to recover is the fact that the sedimentary layer is on average thicker if there are several sedimentary basins a few tens of kilometers wide.

The sediments on the epicontinental Barents Shelf have significantly higher velocities than sediments covering the oceanic crust. This feature of our model can be linked to the uplift of the region in the Neogene and the repeated phases of glaciation in the Barents Sea during the late Pliocene and Pleistocene (Smelror et al., 2009). Uplift and glaciation cause erosion of the sediments covering the Barents Shelf and the deposition of large amounts of young sediments into major submarine fans along the western and northern margin. These young sediments are less consolidated and have as a consequence lower seismic velocities when compared to the older sediments covering the Barents Shelf. The uppermost sediments in the Kara Sea Basin show slightly lower velocities than the uppermost sediments in the East Barents Sea Basin. This correlates with the interpretation that only during the maximum extent of glaciation in the late Pleistocene did the ice sheet reach into the Kara Sea (Smelror et al., 2009). Sediments in the Kara Sea have therefore experienced less erosion, leaving less compacted sediments exposed at the seafloor, possibly together with deposits from other periods of glaciation

6.3.3 Probabilistic earthquake location

The non-linear problem of seismic event location using body wave travel times is often solved using non-linear iterative approaches. A poor station distribution and a complex 3D velocity structure however contribute to the non-linearity of the location problem and create potential instabilities. The potential failure of linearization together with the need for more comprehensive location uncertainty information in the form of a probability density function has led to the formulation of numerous probabilistic approaches (e.g. Kennett and Sambridge, 1992; Billings, 1994; Lomax et al., 2000). Location uncertainty is caused by pick uncertainties (i.e., the inability to accurately estimate onset time for a phase) and uncertainties in the velocity models. Most estimates for location uncertainty do not however take into account the uncertainties in the model used to predict the travel times. They are solely based on pick uncertainties. A probabilistic model, on the other hand, allows a prediction of observables and their uncertainties.

The distribution of an observable (i.e., its value and uncertainty) given a probabilistic model can be recovered by calculating its values for every model belonging to the set of samples that defines the probabilistic model. Similarly it is possible to obtain an estimate for the location uncertainty of a seismic event due to model uncertainty by locating the event for all the models that comprise the posterior set. Here we use an MCMC approach to approximate the posterior distribution for the origin time and location of an earthquake. The maximum of the posterior distribution then defines the hypocenter location and origin time.

We use an earthquake in the western Barents Sea to investigate the influence of model uncertainties on location uncertainties. Figure 6.3.4.a shows the station distribution, and Figure 6.3.4.b the distribution of the mean path velocities, between the event and two selected stations. For longer paths which reside primarily in the mantle, the mean velocity is less influenced than for shorter paths that reside in the crust. We have located the earthquake for each of the models in the posterior distribution. Figure 6.3.4.c shows the 4,000 locations obtained and thereby provides an estimate for the location uncertainty from model errors alone together with an event location obtained using a regional 1D velocity model. All stations available for the location of this event lie to the west of the earthquake. This results in both the error ellipse for the 1D velocity model solution and the cloud of locations being elongated in the west-east direction. We observe a linear trend between late deep event locations to the southwest and early shallow locations to the northeast. Bondár et al. (2004) showed that for an excellent station coverage, depth and origin time are more sensitive to the velocity model than the epicenter

location. We find that for an uneven station distribution as shown here the epicenter location seems to be equally sensitive to the velocity model as to the origin time and depth.

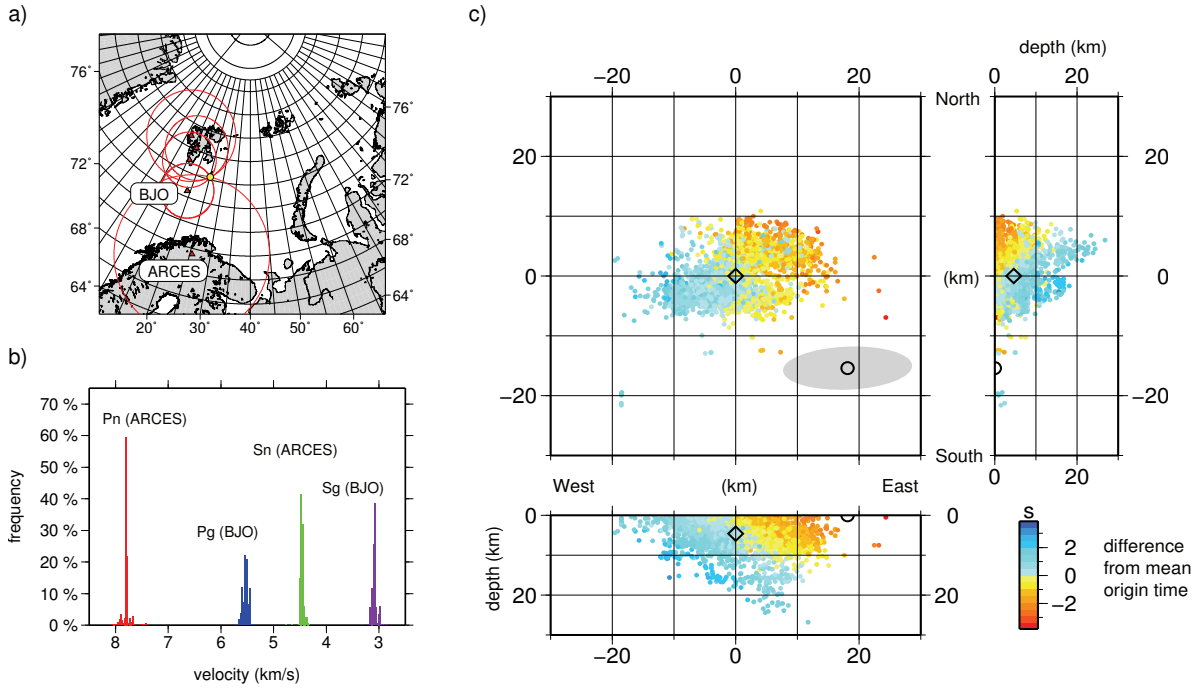

Fig. 6.3.4. Probabilistic location of an earthquake, taking model uncertainties into account: a) station distribution, b) distribution of average path velocities for regional phases for two stations used in the location example and c) hypocenter and origin time of the earthquake computed for each of the models forming our probabilistic model. The mean location is given by the black diamond. The points are colored according to the deviation from the mean origin time of our set of locations. The black circle marks the location of the event computed using a 1D velocity model and a fixed depth of 0 km and the error ellipse is given by the gray shaded area.

6.3.4 Concluding remarks

We have successfully employed a probabilistic approach for the development of a data-driven regional seismic model for the European Arctic. We have compared the mean model of our posterior distribution with other models that cover the region and find that it captures the features that can be resolved with a node spacing of 83 km. Our probabilistic model not only provides images of the subsurface together with estimates of uncertainties, it also allows for the prediction of observables and uncertainties. This can be used to derive seismic event location uncertainties from model uncertainties and can in the future be used for location algorithms that take model uncertainties in addition to uncertainties in onset time into account.

Acknowledgements

We thank NOTUR (The Norwegian Metacenter for Computational Science) and the University of Oslo for providing the computational resource on the Titan III high performance computing facilities. We thank Stephen Myers (LLNL) for contributing the ground Truth data and NGU (The Geological Survey of Norway) for providing the depth to Moho data shown in Figure 6.3.2.d.

Juerg Hauser, NORSAR
Kathleen M. Dyer, LLNL
Michael E. Pasyanos, LLNL
Hilmar Bungum, NORSAR
Jan Inge Faleide, UiO
Stephen A. Clark, UiO
Johannes Schweitzer, NORSAR

References

Bassin, C., G. Laske, and G. Masters (2000). The current limits of resolution for surface wave tomography in North America, EOS Trans. AGU, **81**, F897.

Billings, S. (1994). Simulated annealing for earthquake location, Geophys. J. Int., **118** (3), 680-692.

Bird, P. (2003). An updated digital model of plate boundaries, Geochem. Geophys. Geosyst., **4** (3), 1027.

Bondár, I., S. Myers, E. Engdahl, and E. Bergman (2004). Epicentre accuracy based on seismic network criteria, Geophys. J. Int., **156** (3),483-496.

Ebbing, J., C. Braitenberg and S. Wienecke (2007). Insights into the lithospheric structure and the tectonic setting of the Barents Sea region by isostatic considerations, Geophys. J. Int., **171**, 1390-1403.

Kennett, B. L. N. and M. Sambridge (1992). Earthquake location - genetic algorithms for teleseismic location, Phys.Earth Planet. Inter., **75** (1-3), 103-110.

Lomax, A., J. Virieux, P. Volant, and C. Berge (2000). Probabilistic earthquake location in 3D and layered models: Advances in Seismic Event Location, pp. 101-134.

Ritzmann, O., N. Maercklin, J. I. Faleide, H. Bungum, W. D. Mooney and S. T. Detweiler (2007). A 3D geophysical model for the crust in the greater Barents Sea region: Model construction and basement characterization. Geophys. J. Int., **170,** 417-435.

Smelror, M. O., O. Petrov, G. B. Larsen and S.Werner (2009). Geological History of the Barents Sea, Geological Survey of Norway.